Research Progress in Mechanical and Manufacturing Engineering Vol. 3 No. 1 (2022) 1009-1019

RPMME

Homepage: http://publisher.uthm.edu.my/periodicals/index.php/rpmme
e-ISSN : 2773-4765

Thermal Energy Harvesting: Parameter Tuning of Maximum Power Point Tracking Algorithm for Real-Time Temperature Data from Solar Irradiance

Muhammad Nazri Rejab[1], Omar Mohd Faizan Marwah[1*], Muhammad Akmal Johar[1]

[1]Faculty of Mechanical and Manufacturing Engineering,
Universiti Tun Hussein Onn Malaysia, Parit Raja, Batu Pahat, 86400, MALAYSIA

* Corresponding Author Designation

DOI: https://doi.org/10.30880/rpmme.2022.03.01.106
Received 01 Dec 2021; Accepted 01 April 2022; Available online 30 July 2022

Abstract: Thermal energy becomes priceless renewable energy due to the impoverishment of fossil fuels and the increasing carbon pollution. Implementing the thermoelectric generator (TEG) in a real-time temperature gradient calls for the intensive appraisal of the energy management circuit to accomplish the maximum power transfer from the thermal source to the output load. Successful implementation of the TEG relies on the MPPT algorithm to confirm the maximum power point achievement at a particular thermal energy level. In-depth analyses for the most acceptable MPPT algorithm methods are convenient to the TEG realistic behavior. Perturb and Observe (P&O) and Incremental Conductance (INC) MPPT algorithms are popular in thermal energy harvesting. Therefore, the comparison between these two (2) MPPT algorithms in TEG raised to study the efficiency, power losses, and oscillation range based on the parameter tuning results. Furthermore, the qualification of this MPPT algorithm in conjunction with the real-time temperature changes due to solar irradiance is evaluated. P&O shows potential to achieve the MPPT, but INC gives superior capability regarding the TEG implementation at rapid temperature changes. Thereby, the design and development of a thermal energy harvesting circuit based on the evaluation of two MPPT algorithms for real-time temperature different from solar irradiance encourage to be done.

Keywords: Thermoelectric Generator (TEG), Perturb And Observe, Incremental Conductance, Real-Time Temperature, Roof And Attic Area.

1.0 Introduction

Malaysia is exposed to solar irradiance from 4.21 kWh/m^2 to 5.56 kWh/m^2 [1][2]. Generally, a roof is a surface directly exposed to solar irradiance and capable of storing thermal energy due to the low albedo characteristic of roof material. Thereby, harvesting thermal energy in Malaysian residential

**Corresponding author: mdfaizan@uthm.edu.my*

housing is feasible and practical [1]. Compared to solar energy, the advantage of thermal energy is that it is available for 24 hours. In addition, to harvesting the thermal energy, a thermoelectric generator (TEG) is an ideal candidate to convert thermal energy into electrical energy via the Seebeck effect. The efficiency of TEG is interrelated to the impedance matching between the TEG module internal resistance, R_{in} and the load variation, $R_{L,}$ to achieve optimum power transfer [3][4]. In addition, temperature fluctuation also affects the TEG module performance to obtain the maximum power point (MPP) [5]. Referring to Figure 1, the MPP is achieved at a half value of both short circuit current (I_{SC}) and open-circuit voltage (V_{OC}) of the TEG. In addition, the linear voltage and current depend on the load resistance variation (R_L). At the variable temperature difference (ΔT), the maximum power point is shown by the dashed line in Figure 1. In addition, the cross point between the power curve from the TEG and the MPPT define as matched load, where the TEG internal resistance is equal to the load resistance ($R_{in} = R_L$). Therefore, the maximum power point tracking (MPPT) algorithm is introduced with the thermal energy harvesting system to obtain the MPP. Several approaches of the MPPT algorithm, such as Perturb and Observe (P&O) and Incremental Conductance (INC), are used.

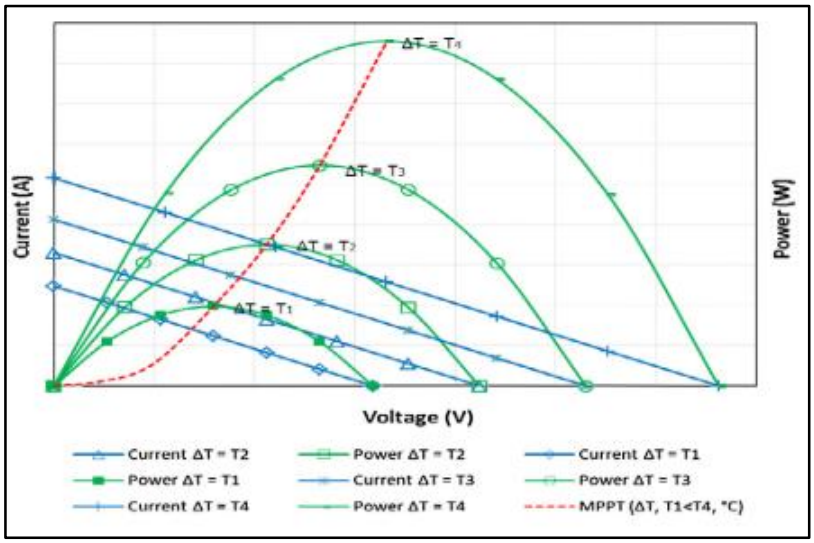

Figure 1 TEG V-I, P-V and MPPT curve at a specific temperature different [6]

P&O provides a simple algorithm, lower cost, and uncomplicated troubleshooting. However, the drawback of this algorithm is the energy losses caused by the oscillation of the operating point around MPP. Thereby, tuning the perturbation step can mitigate the problem for new MPP with sudden temperature changes. However, the generalisability of published research for P&O algorithm issues is problematic in determining the proper configuration to reduce losses due to inefficient step size, power factor, synchronization, load matching, and input energy requirement [7][8][9][10]. At the same time, the INC algorithm is still used in practice due to its simplicity, economical [11][12], and satisfactory performance with experimental implementation on microcontrollers [13][14]. However, the INC algorithm demands proper tuning according to the type of application, parameter range, response time, and input signal conditions. The tuning procedure involved adjusting step size to increase speed and tracking accuracy by reducing the iteration of tracking the present voltage[15]. Furthermore, the MPPT frequency has the same magnitude as the temperature time constant of the TEG to improve the MPPT accuracy [16][17].

Therefore, this research focuses on tuning the frequency and duty cycle step-size of both MPPT algorithms to obtain the MPP at real-time temperature data. The performance of the MPPT algorithm is evaluated based on the efficiency, power losses, and oscillation range. Section 2 explains the real-time temperature measurement and simulation with proposed synchronous data management and absolute data analysis. Further, the parameter tuning result is discussed in section 3. Finally, the

parameter tuning of both MPPT algorithms for the TEG energy harvesting system to harvest thermal energy based on real-time temperature data is concluded.

2.0 Materials and Methods

This section explains all methods involved in the research. It is divided into experimental temperature setup, real-time simulation, and the fundamental of MPPT subsections.

2.1 Experimental temperature measurement setup

The TEC1-12706 TEG module (TEM) arrangement at the rooftop is present in Figure 2 (A). 192 TEM connected with the equivalent amount of TEM in parallel array configuration covered $1m^2$, sandwiched between the metal deck roof and the heatsink. Aluminium heatsinks were used for heat dissipation and increased cooling efficiency using natural cooling from the wind blowing. Thermal paste (Cooler master HTK-002) is used between both sides of TEM. Moreover, the pyranometer was used to record the solar irradiance value along with the experiment. K-type thermocouples were used to measure temperature at the hot and cold sides of TEM and ambient. Experiment data consists of the temperature of both TEM sides, voltage, and current recorded simultaneously using National Instrument (NI) data acquisition. The NI system used is illustrated in Figure 2: TEM (**A) experimental setup (B) NI data acquisition system**

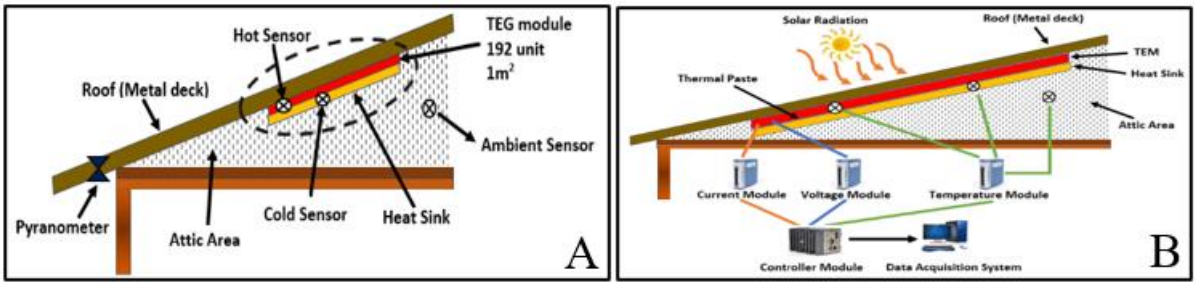

Figure 2: TEM (A) experimental setup (B) NI data acquisition system

Labview software is integrated with the data program layout in

Figure **3**.

Figure **3**(A) is the TEM block setup, and

Figure **3**(B) is the programming layout to record and synchronize all the experiment data in the computer. Experiment data was recorded for 20 days at every second interval for 24 hours.

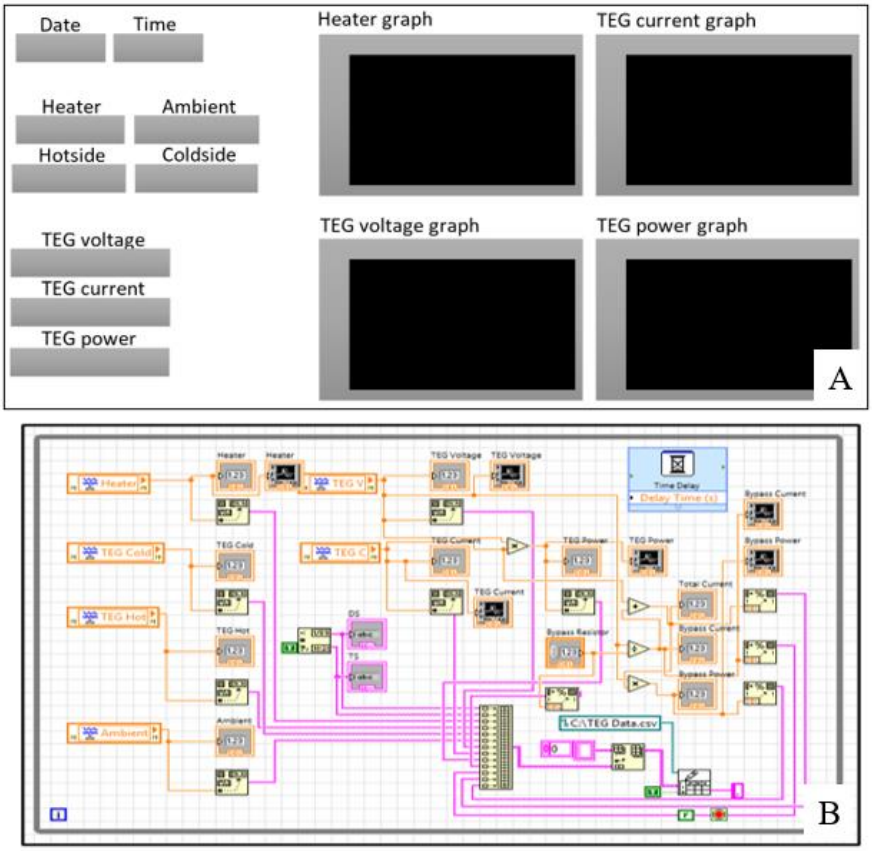

Figure 3: Labview software *layout* (A) *Blo*ck (B) Programme

2.2 Real-time simulation

Matlab Simulink software was used to evaluate the frequency and duty cycle of the MPPT algorithm for real-time temperature data. The rapid fluctuation of the temperature data needs data analysis tools to accommodate the transition of input and output results changing. Therefore, synchronous data management records simultaneous input and output results, as in Figure 4. The advantage of this method is recording the MPPT value's transition for different frequency and duty cycle step-size values. In addition, the data analysis reduced the error.

Further, the reverse condition occurs where the hot side becomes the cold side and vice versa for the 24 hours data. This condition indicated the polarity changing at a certain point depending on the weather and solar irradiance. Therefore, absolute data analysis introduces to deal with this condition for further investigation of all the real-time temperature data.

The input voltage from the TEG is usually low. Therefore, the DC converter increases the input voltage from the TEG using the MPPT algorithm to track and control the MOSFET to obtain the MPP. The component used in the converter is the inductor (100µH), MOSFET (IRLZ44N), diode (IN5817) and capacitor (47µF).

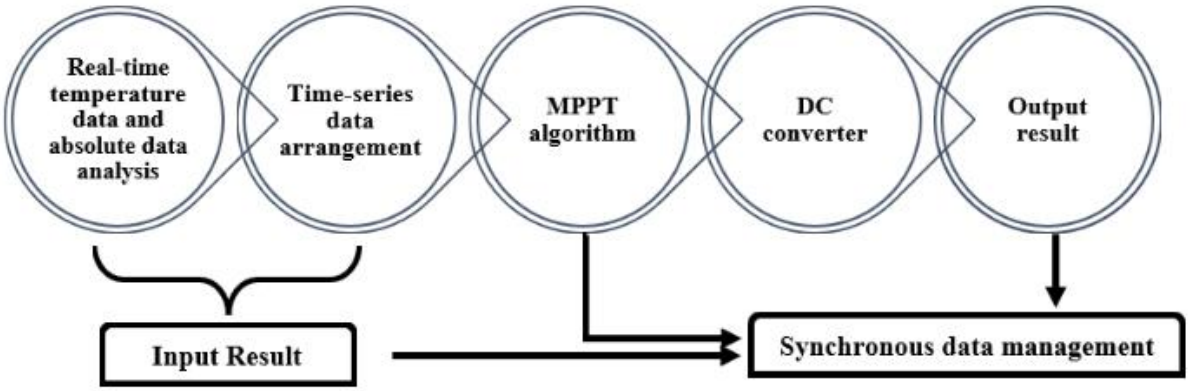

Figure 4: The real-time data simulation step

2.3 Fundamental of MPPT algorithm

This section briefly introduced the working principle of the P&O and INC MPPT algorithm to obtain the MPP.

2.3.1 Perturb and Observe

P&O algorithm traces the power output from the present value and compares it with the future value to determine the rising or falling of voltage and current from the TEG. Based on this technique, the set of voltage and current was taken as a reference value for predicting the future operating point of the MPPT. The voltage and current are constantly regulated at dynamic and steady-state oscillation [18][19]. The conventional P&O algorithm flow chart is presented in Figure 5(B). The algorithm performance hinged on the duty cycle step-size of the converter for alluring a superior MPP. In addition, this was achieved through continuous perturbation present voltage of the thermal source. The principle operation focuses on perturbating the input voltage from the TEG towards the maximum power point until dP/dV>0 [20]. Afterwards, the algorithm keeps tracking in the same direction until dP/dV<0, the perturbation inverts the tracking direction due to the changing direction of the maximum power point. The maximum power point occurs when the dP/dV=0. The illustration of the operation of the MPPT algorithm shows in Figure 5 (A).

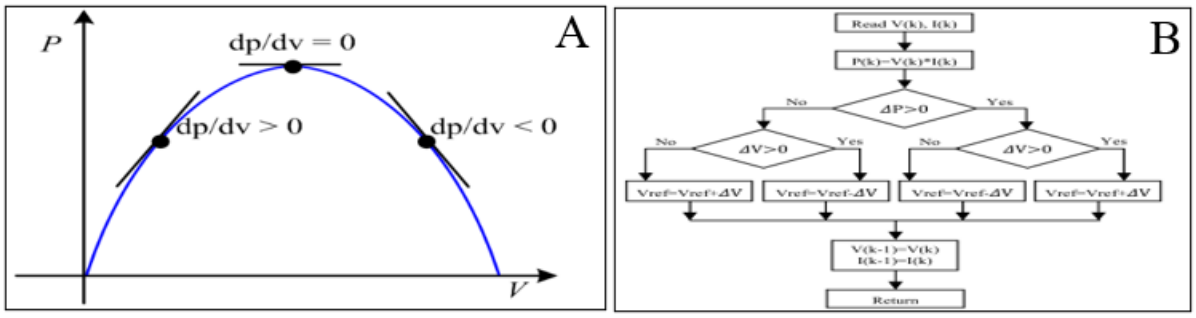

Figure 5: P&O MPPT algorithm (A) Tracking curve (B) Flowchart

2.3.2 Incremental Conductance

INC MPPT algorithm is classified as a direct method to trace the MPPT due to the simple algorithm structure and low tracking time [21]. INC MPPT algorithm compares the present conductance value (I/V) to adjust the conductance value (ΔI/ΔV) to obtain the maximum power tracking [22][23][19][24]. Derivation for this method is described in Eq. 1.

$$dP/dV = 0; \text{ at MPP} \qquad \text{Eq. 1}$$

$$dP/dV > 0; \text{ left curve of MPP}$$

$$dP/dV < 0; \text{ right curve of MPP}$$

The input voltage, V and input power, P relationship expressed by Eq. 2.

$$dP/dV = d(IV)/dV = I + V(dI/dV) \quad \text{Eq. 2}$$

$$\approx I + V\,(\Delta I/\Delta V)$$

Therefore, the MPP curve follows the Eq. 3.

$$\Delta I/\Delta V = -(I/V); \text{ at MPP} \quad \text{Eq. 3}$$

$$\Delta I/\Delta V > -(I/V); \text{ at left curve of MPP}$$

$$\Delta I/\Delta V < -(I/V); \text{ at right curve of MPP}$$

While for the INC MPPT algorithm flowchart is presented in Figure 6.

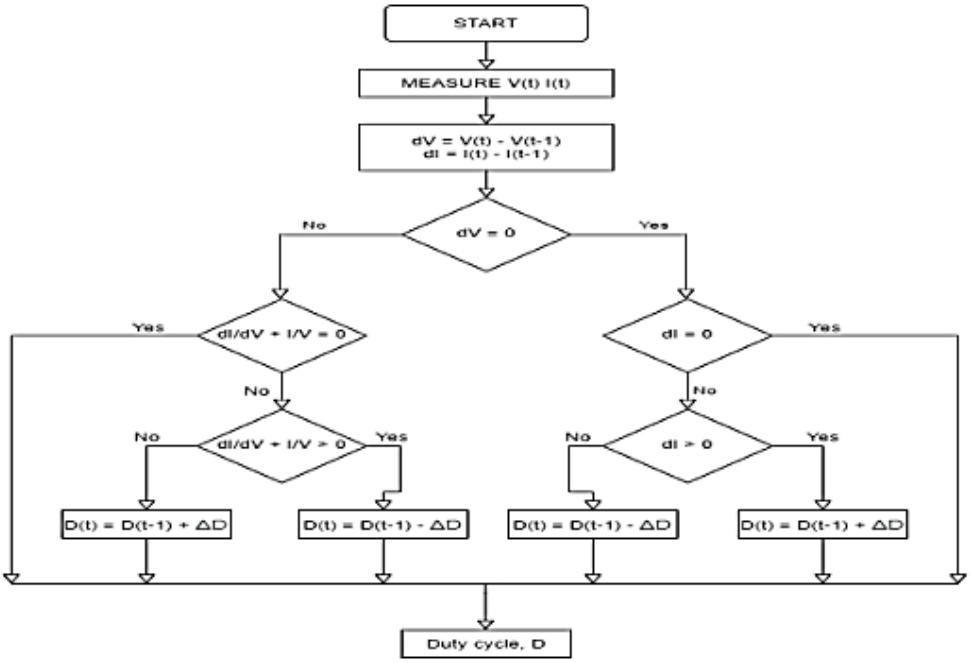

Figure 6: The INC MPPT algorithm flowchart

3.0 Results and Discussion

This section presents data and analysis of the research work. First, two parameters are involved in the analysis: frequency and duty cycle step size. Then, compare two MPPT algorithms based on the criteria to evaluate the tracking behaviour to obtain the MPP.

3.1 Frequency tuning

Figure 7 presents the frequency tuning for the INC MPPT algorithm. Compared to all the frequencies, a significant effect observes the transition response. Lower frequency shows the high oscillation, thereby reducing the power tracking efficiency. In terms of MPP tracking, this condition should avoid because of the high-power losses. On the contrary, the oscillation reduces when the frequency value increases. Response time also can be evaluated for each frequency to achieve the MPP. High frequency gives a better result to adapt to the rapidly changing. On average, the response time for all the frequency ranges is 3 mSec. The transition response for all frequencies is no overshoot, excluding the 10 kHz and 15 kHz at the beginning of the MPP. The evaluation result for INC frequency is listed in Table 1.

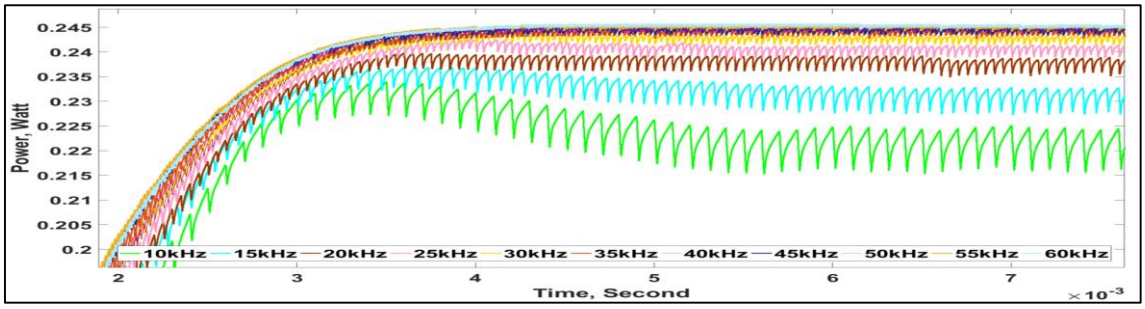

Figure 7: INC frequency response

Table 1: The overall result for the INC evaluation criteria

Frequency,kHz	10	15	20	25	30	35	40	45	50	55	60
Efficiency, %	82.82	83.32	83.85	84.07	84.34	84.51	84.54	84.56	84.60	84.63	84.70
Oscillation range, x10^{-3}	9.7	5.5	3.7	3.1	1.9	1.8	1.4	1.4	1.1	1.2	1.2

The P&O MPPT algorithm to track the MPP is illustrated in Figure 8. The same behaviour was observed in the frequency value's effect on tracking the MPP. The low-frequency value shows high oscillation compared to the high-frequency value. At the beginning of MPP tracking, overshoot occurs and nonstable conditions from 0 mSec to 2.5 mSec. Therefore, it will affect the MPP value under rapid conditions. Thereby should be avoided to use in the real-time simulation. Table 2 lists the overall result for the performance evaluation of the P&O algorithm.

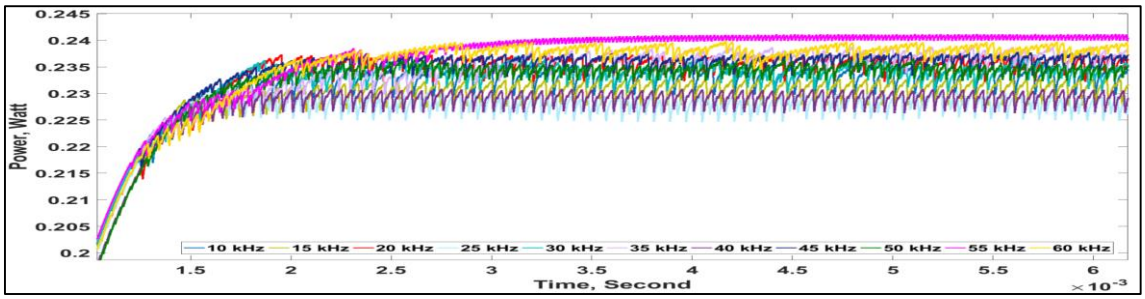

Figure 8: P&O frequency response

Table 2: The overall result for the P&O evaluation criteria

Frequency,kHz	10	15	20	25	30	35	40	45	50	55	60
Efficiency, %	82.82	83.32	83.85	84.07	84.34	84.51	84.54	84.56	84.60	84.63	84.70
Oscillation range, x10^{-3}	5.6	4.9	5	5.7	7.1	4.9	4.5	4.4	3.1	1.2	6.5

Figure 9 compares P&O and INC at 0.0002 and 0.002 duty cycle step-size values. Interestingly, the result indicates a similar response despite the different frequency and MPPT algorithm used. P&O algorithm at 55 kHz obtain the MPP similar transition response to the INC 60 kHz, but with higher oscillation. In addition, the response time for both algorithms only needs 4.164 mSec to achieve 0.2453 watts of MPP. Moreover, the P&O algorithm at 60 kHz shows a similar response to INC at 55 kHz to obtain the MPP. At point (A), INC at 55 kHz shows less oscillation than P&O at 60 kHz. Refer to Table 3, the comparison of evaluation criteria between both MPPT algorithms.

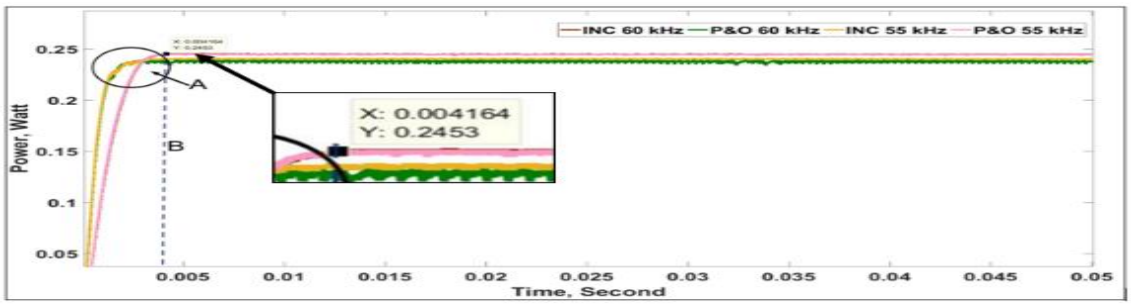

Figure 9: P&O and INC frequency response comparison at the same frequency

Table 3: The frequency comparison results for both MPPT algorithm

MPPT algorithm	P&O		INC	
Frequency, kHz	55	60	55	60
Efficiency, %	84.53	84.70	84.63	84.70
Oscillation range, x10^{-3}	1.2	6.5	1.2	1.2

3.2 Duty cycle step size tuning

Figure 10 portrays the transition response of the INC algorithm. The effect of duty cycle step-size on the response time is observed. A low value of 0.0001 presents a large offset and response time. It takes approximately 15 mSec to reach a steady state. Thereby not suitable to use for real-time tracking. The response time decrease when the duty cycle step-size increase, thus increasing the efficiency and reducing the oscillation. Duty cycle step-size values at 0.004 and 0.002 can achieve the steady-state at 2 mSec.

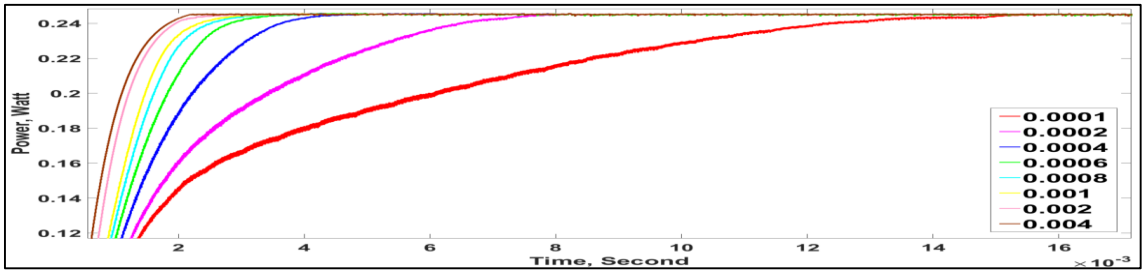

Figure 10: INC duty cycle step-size response

Table 4: INC duty cycle step-size evaluation result

Duty cycle step-size, x10^{-3}	0.1	0.2	0.4	0.6	0.8	1	2	4
Efficiency, %	83.89	84.39	84.63	84.68	84.75	84.76	84.80	84.86
Power losses, %	4.09	4.09	4.08	4.07	4.06	4.08	4.08	4.08

Further, the duty cycle step-size transition for P&O is shown in Figure 11. The oscillation is higher compared to the INC. The oscillation was observed for the 0.1 to 0.02 duty cycle step-size value. In addition, the oscillation begins to build at the response time range from 1 to 2 mSec until it gains the constant state. Interestingly, the 0.0002 has two behaviours: the offset and low response time compared to other duty cycle step-size values. It needs approximately 3.5 mSec to obtain the steady-state. 0.06, 0.04, and 0.08 values show high oscillation, thus not recommended as the duty cycle step-size in the MPPT algorithm. The result is similar to 0.02, but the oscillation is smaller than the previous value. Therefore, 0.002 is the ideal duty cycle step-size value because it has low oscillation and response time.

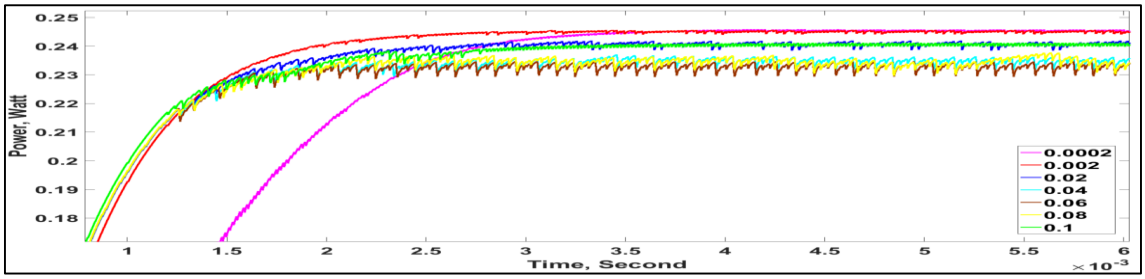

Figure 11: P&O Duty cycle step-size response

Table 5: P&O duty cycle step-size evaluation result

Duty cycle step-size, x10^{-3}	0.2	2	20	40	60	80	100
Efficiency, %	84.75	84.83	83.98	83.35	83.21	83.26	83.80
Power losses, %	4.07	4.10	4.46	4.95	5.19	4.84	4.55

Furthermore, comparing the same frequency and duty cycle step size for both MPPT algorithms gives an exciting result, as presented in Figure 12. The highest offset occurs for 60 kHz INC with 0.0002 duty cycle step-size, followed by P&O at the same duty cycle value. The 0.002 duty cycle step-size value obtains similar behaviour between the P&O algorithm at 55 kHz and the INC algorithm at 60 kHz. In detail analysis at (A), the oscillation range for INC algorithm is better than P&O with slightly different. Each algorithm is the same response time from the beginning to track the MPP. In terms of power losses, the INC is better than P&O. It indicates an alternative to choose either P&O or INC can be used as the MPPT algorithm to track MPP for thermal energy harvesting. Table 6 lists the comparison data for MPPT algorithms.

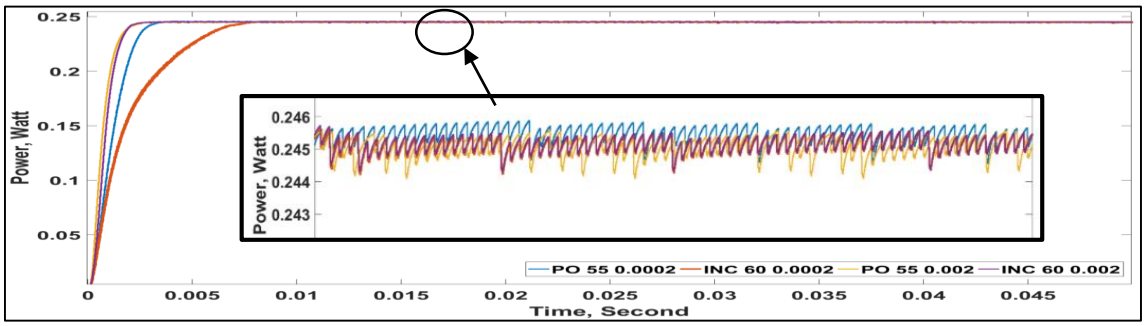

Figure 12: Comparison between P&O and INC at 0.0002 and 0.002 duty cycle step-size and frequency at 50 kHz and 60 kHz

Table 6: The duty cycle step-size comparison results for both MPPT algorithm

MPPT algorithm	P&O	INC	P&O	INC
Duty cycle step-size value, x10^{-3}	0.2		2	
Frequency, kHz	55	60	55	60
Efficiency, %	84.75	84.39	84.83	84.80
Oscillation range, x10^{-3}	4.07	4.09	4.10	4.08

4.0 Conclusion

The performance of the TEG to harvest the thermal energy from solar radiation at the roof and attic area confide in the capability of the MPPT algorithm to track the MPP. This study evaluated the effect

of frequency and duty cycle step-size based on the real-time temperature data. The findings indicate that lower frequency values contributed to high oscillation. Thereby deteriorating the efficiency of tracking the MPP. P&O algorithm obtains high efficiency at 55 kHz with 84.63% efficiency and an oscillation range of 0.0012. While the INC algorithm reaches the MPP at 60 kHz with 84.70% efficiency and a similar oscillation range of P&O. The comparison between both MPPT algorithms indicates a similar response time; P&O 55 kHz with INC 60 kHz and P&O 60 kHz with INC 55 kHz. The output power of INC at 60 kHz is 0.2391 Watt, and at 55 kHz is 0.2374 Watt. In addition, the P&O obtained 0.2352 Watt at 55 kHz and 0.2389 Watt at 55 kHz. The comparison of frequency tuning results shows that the INC algorithm is better than P&O.

Furthermore, the duty cycle step-size has also shown a significant effect on gaining the MPP. The 0.004 value of the INC algorithm earns the highest efficiency at 84.86%, with 4.08% of power losses. On the other hand, the P&O algorithm efficiency is 84.83%, with 4.10% power losses at a 0.002 duty cycle step-size value. Comparing the duty cycle step-size of 0.0002 and 0.002, the P&O is better than INC. The P&O and INC parameter tuning findings have significant implications for understanding how the frequency and duty cycle step-size response tracks the MPP based on real-time temperature data. Therefore, this research provides insights for further study in designing and developing a real-time thermal energy harvesting system to harvest thermal energy at 24 hours.

Acknowledgement

The research was mainly supported by the Ministry of Higher Education (MOHE) through Fundamental Research Grant Scheme (FRGS/1/2018/TK10/UTHM/02/2) or Vot No. K108.

References

[1] N. M. Shatar *et al.*, "Performance evaluation of unconcentrated photovoltaic-thermoelectric generator hybrid system under tropical climate," *Sustain.*, vol. 11, no. 22, 2019.

[2] Y. Y. Lee, M. F. Md Din, K. Iwao, Y. H. Lee, and N. Anting, "Impact of thermal behaviour of different environmental conditions on ambient environment and thermal discomfort in Malaysia," *Indoor Built Environ.*, vol. 0, no. 0, pp. 1–15, 2020.

[3] T. C. Watson, J. N. Vincent, and H. Lee, "Effect of DC-DC voltage step-up converter impedance on thermoelectric energy harvester system design strategy," *Appl. Energy*, vol. 239, no. August 2018, pp. 898–907, 2019.

[4] H. Mamur and Y. Çoban, "Detailed modeling of a thermoelectric generator for maximum power point tracking," *Turkish J. Electr. Eng. Comput. Sci.*, vol. 28, no. 1, pp. 124–139, 2020.

[5] S. Mahmoudinezhad, P. A. Cotfas, D. T. Cotfas, L. A. Rosendahl, and A. Rezania, "Response of thermoelectric generators to Bi2Te3 and Zn4Sb3 energy harvester materials under variant solar radiation," *Renew. Energy*, vol. 146, pp. 2488–2498, 2020.

[6] S. Twaha, J. Zhu, Y. Yan, B. Li, and K. Huang, "Performance analysis of thermoelectric generator using dc-dc converter with incremental conductance based maximum power point tracking," *Energy Sustain. Dev.*, vol. 37, pp. 86–98, 2017.

[7] K. Yahya, M. Z. Bilgin, T. Erfidan, and B. Çakir, "Improving the performance of the MPPT for thermoelectric generator system by using Kalman filter," *2018 5th Int. Conf. Electr. Electron. Eng. ICEEE 2018*, pp. 129–132, 2018.

[8] O. Lopez-Lapena, M. T. Penella, and M. Gasulla, "A closed-loop maximum power point tracker for subwatt photovoltaic panels," *IEEE Trans. Ind. Electron.*, vol. 59, no. 3, pp. 1588–1596, 2011.

[9] L. Hou and W. Chen, "A novel MPPT method for autonomous wireless sensor networks node with thermal energy harvesting," *Eng. Res. Express*, vol. 2, no. 1, 2020.

[10] E. A. Man, D. Sera, L. Mathe, E. Schaltz, and L. Rosendahl, "Dynamic Performance of Maximum Power Point Trackers in TEG Systems Under Rapidly Changing Temperature Conditions," *J. Electron. Mater.*, vol. 45, no. 3, pp. 1309–1315, 2016.

[11] A. N. M. Mohammad, M. A. M. Radzi, N. Azis, S. Shafie, and M. A. A. M. Zainuri, "An enhanced adaptive perturb and observe technique for effcient maximum power point tracking under partial shading conditions," *Appl. Sci.*, vol. 10, no. 11, 2020.

[12] P.-C. Chen, P.-Y. Chen, Y.-H. Liu, J.-H. Chen, and Y.-F. Luo, "A comparative study on maximum power point tracking techniques for photovoltaic generation systems operating under fast changing environments," *Sol. Energy*, vol. 119, pp. 261–276, 2015.

[13] D. Mustafic, D. Jokic, S. Lale, and S. Lubura, "Implementation of Incremental Conductance MPPT Algorithm in Real Time in Matlab/Simulink Environment with Humusoft MF634 Board," *2020 9th Mediterr. Conf. Embed. Comput. MECO 2020*, pp. 8–11, 2020.

[14] L. Zhang, S. S. Yu, T. K. Chau, T. Fernando, and H. H. C. Iu, "An advanced incremental conductance MPPT technique considering time-varying solar irradiances," *IOP Conf. Ser. Earth Environ. Sci.*, vol. 322, no. 1, 2019.

[15] H. Islam *et al.*, "Performance evaluation of maximum power point tracking approaches and photovoltaic systems," *Energies*, vol. 11, no. 2, pp. 7–9, 2018.

[16] P. Cao, Y. Qian, P. Xue, D. Lu, J. He, and Z. Hong, "A Bipolar-Input Thermoelectric Energy-Harvesting Interface with Boost/Flyback Hybrid Converter and On-Chip Cold Starter," *IEEE J. Solid-State Circuits*, vol. 54, no. 12, pp. 3362–3374, 2019.

[17] M. Compadre Torrecilla, A. Montecucco, J. Siviter, A. R. Knox, and A. Strain, "Novel model and maximum power tracking algorithm for thermoelectric generators operated under constant heat flux," *Appl. Energy*, vol. 256, no. September, p. 113930, 2019.

[18] F. L. Tofoli, D. de Castro Pereira, and W. J. de Paula, "Comparative study of maximum power point tracking techniques for photovoltaic systems," *Int. J. Photoenergy*, vol. 2015, 2015.

[19] M. L. Azad, P. K. Sadhu, and S. Das, "Comparative Study between PO and Incremental Conduction MPPT Techniques- A Review," *Proc. Int. Conf. Intell. Eng. Manag. ICIEM 2020*, pp. 217–222, 2020.

[20] M. A. A. Faria, P. A. J. Stecanella, E. G. Domingues, P. H. G. Gomes, W. P. Calixto, and A. J. Alves, "Modeling, simulation and control of a thermoelectric generator," in *2015 IEEE 15th International Conference on Environment and Electrical Engineering, EEEIC 2015 - Conference Proceedings*, 2015.

[21] S. Lalouni, D. Rekioua, K. Idjdarene, and A. Tounzi, "Maximum power point tracking based hybrid hill-climb search method applied to wind energy conversion system," *Electr. Power Components Syst.*, vol. 43, no. 8–10, pp. 1028–1038, 2015.

[22] J. W. Simatupang and I. Purnama, "Study on Various Simple Power Tracking Methods for Thermoelectric Generator," *Proceeding - 2019 Int. Conf. Sustain. Energy Eng. Appl. Innov. Technol. Towar. Energy Resilience, ICSEEA 2019*, no. 1, pp. 79–84, 2019.

[23] S. Motahhir, A. El Hammoumi, and A. El Ghzizal, "The most used MPPT algorithms: Review and the suitable low-cost embedded board for each algorithm," *J. Clean. Prod.*, vol. 246, p. 118983, 2020.

[24] R. R. Sahoo, R. R. Sahool, and M. Singh, "Analysis of Variable Step Incremental Conductance MPPT Technique for PV System," *IOSR J. Electr. Electron. Eng.*, vol. 11, no. 2, pp. 41–48, 2016.